

We\_R04\_03

## Imaging Paleocene and Jurassic Prospects Within the Porcupine Basin, Ireland: A Case Study

M. Hart<sup>1\*</sup>, E. Cho<sup>1</sup>, S. Bhambher<sup>1</sup>, A. Hulks<sup>1</sup>, S. O'Keefe<sup>1</sup>

<sup>1</sup> TGS

### Summary

We present a case study and outline the workflow used to process 5500 km<sup>2</sup> of new seismic data in the Porcupine Basin area of the Celtic Sea, with a triple-source acquisition configuration.

Key processing challenges include the imaging of faults in the Jurassic interval, volcanic sills and the high velocity Cretaceous chalk. In addition to these processing challenges, several shallow-gas pockets and channels with variable-velocity infill require detailed depth-velocity modelling to resolve deflections in the underlying sediments.

A processing flow is presented to address these imaging challenges, along with those posed by the triple-source acquisition configuration. This flow includes deblending, multiple attenuation, regularisation and incorporated FWI along with high-resolution image-guided tomography to produce an accurate velocity model for prestack depth migration.

Improved imaging of the complex and potentially prospective structures found within the Porcupine Basin is achieved. Detailed anomalies such as shallow channels and gas clouds are corrected with a combination of high-resolution tomography and FWI, which gives increased confidence in the positioning of events along the underlying sediments.

## Introduction

During 2017, we acquired approximately 5500 km<sup>2</sup> of new seismic data in the Porcupine Basin area of the Celtic Sea, with a triple-source acquisition configuration. 960 km<sup>2</sup> of vintage data were merged into this project and the whole reprocessed as a single volume (Figure 1)

The Porcupine Basin is a failed symmetrical rift basin and is typified by several large-scale rotated fault blocks, offsetting Middle Jurassic strata and covered by the synrift Upper Jurassic section. Several hydrocarbon plays have been defined within the post rift succession, such as the Paleocene basin-floor channel system with the “Avalon” prospect and the Lower Cretaceous Drombeg prospect. There are many identified leads just above and below the Cretaceous Chalk along the western basin flank. The tilted fault blocks in the north of the Porcupine Basin, spanning across the west in the Porcupine High and East in the Celtic Platform, offer an insight into the continuation of the faulting within Lower Cretaceous sections.

This paper will briefly describe the acquisition configuration and processing flow that was developed to address the imaging challenges posed by this geology. Particular attention will be paid to the production of the depth velocity model and its role in correctly positioning the deep sediments.

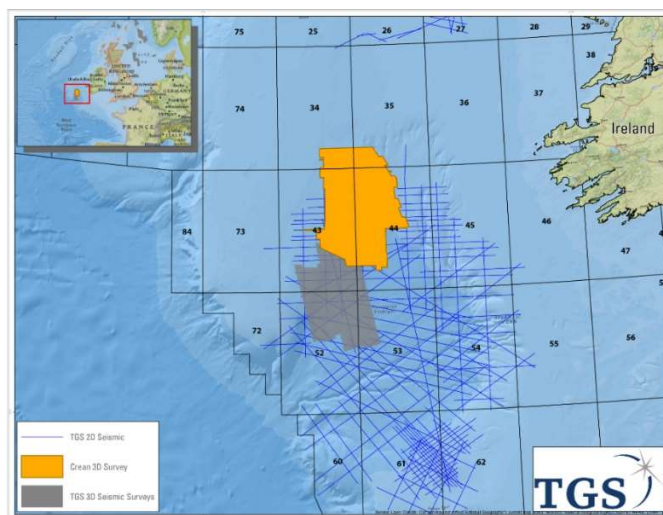


**Figure 1** Crean 3D survey location in the Celtic Sea.

## Addressing Imaging Challenges

Key processing challenges in the area include those posed by the triple source acquisition and the imaging of: faults in the Jurassic interval, volcanic sills and Cretaceous carbonate layers. Of specific interest are the high velocity Cretaceous Chalk units and the sediments just above and below are of particular importance. In addition to these processing challenges, several shallow gas pockets and channels with variable velocity infill require detailed depth-velocity modelling to resolve pull ups in the underlying sediments. The flow designed to meet these challenges can be summarised as: deblending, multiple attenuation, regularisation and full waveform inversion (FWI), along with high-resolution image-guided tomography prior to prestack depth migration.

## Triple Source Acquisition and Deblending

Higher resolution seismic can be acquired without reducing the cable spacing by increasing the number of sources from two to three. The shot interval is reduced to maintain CMP fold, resulting in an overlap with the previous (S1), current (S2) and next (S3) shot records. A multidomain coherency-based deblending workflow as described by Baldock et al. (2018) is used to separate the overlapping shot records. The blended energy in certain domains is incoherent due to both random and natural timing

variations. The deblending workflow utilises incoherency to remove the strong amplitude S3 data without harming the weaker underlying S2 data (Figure 2). A grid spacing of 6.25 m x 18.75 m was achieved with this method, without increasing the acquisition costs.

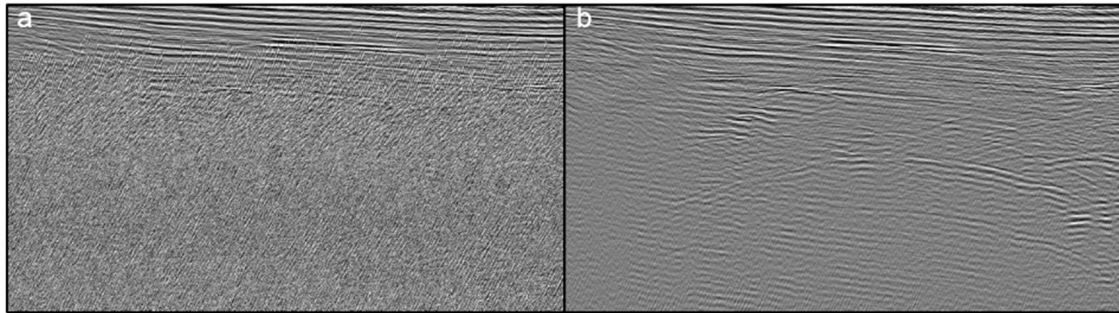


**Figure 2:** Stack before (a) and after (b) deblending.

### Multiple Attenuation

Surface-related multiples can be predicted for a given target trace by a multidimensional convolution of 3D shot and receiver gathers (Berkhout and Verschuur 1997). This process is referred to as surface related multiple elimination (SRME). For conventional narrow-azimuth marine acquisition, shot and receiver sampling is never dense enough for optimal SRME multiple prediction without first applying some form of regularisation. Testing suggests that SRME benefits from the improved shot sampling of the triple-source acquisition. However, it is still necessary to apply some regularisation to take care of coverage holes, missing near offsets on the outer cables and empty subsurface bins caused by cable feathering. These coverage holes, if not counteracted, reduce the quality of the multiple model. The regularisation used is an antileakage Fourier transform (4D ALFT) which enables the SRME to accurately predict the multiples, which are then subtracted from the unregularised input data. This data is then further processed to reduce noise and ameliorate remaining interbed multiples.

### Regularisation

After the full sequence of preprocessing low-fold areas and offset irregularities are addressed with 4D antileakage Fourier transform (ALFT). The ALFT approach uses a matching-pursuit technique that iteratively claims the strongest plane-wave components in each iteration (Whiteside et al. 2014). The four-dimensional aspect of the process allows information for adjacent offsets, as well as information from adjacent bins, to be used to estimate missing traces.

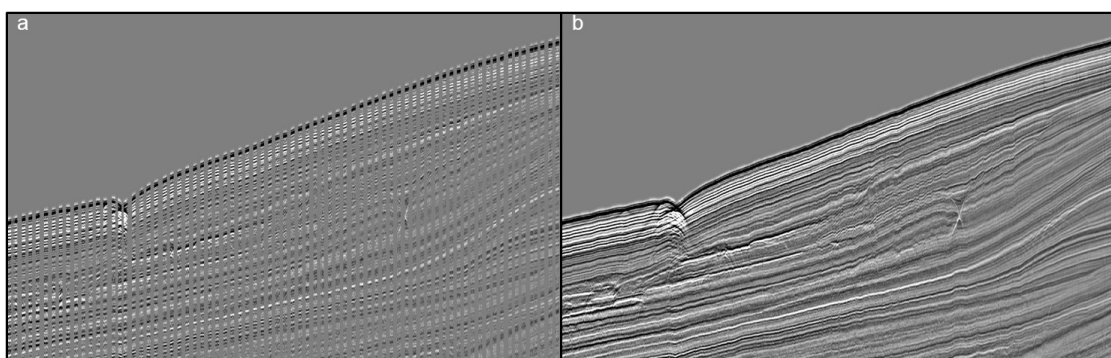


**Figure 3:** 331 m offset plane before (a) and after (b) regularisation.

Antileakage regularisation better preserves dips and diffraction energy when regularising the data. Using neighbouring offsets to reconstruct traces and honouring offset and azimuthal components mean that these traces are well behaved and provide good seismic correlation with surrounding bins (Figure 3). The demultiple data with accurately reconstructed near offsets are a good starting point for detailed depth velocity model building.

## Image Guided Tomography

Depth velocity model building and Kirchhoff depth migrations address the challenges of correctly positioning the Jurassic fault blocks and resolving undulations across the target Druid and Top Chalk horizons by correctly modelling velocity variations across the overlying Eocene channel structures.

A detailed velocity model is built, incorporating image-guided tomography (IGT) and offset-dependent picking. Model building is performed in a top-down, layer-stripping approach, where early iterations concentrated on the shallow post-chalk sediments, which included the Eocene channels. The chalk layer is then incorporated, before moving down to the underlying Cretaceous and more complex Jurassic geology. Horizon-based constraints applied during model building prevent leakage of updates across the high-contrast Top Chalk boundary. Localised details such as gas clouds are identified with interpretation-driven modelling (IDM) - interpreted horizons are incorporated into the high-resolution tomography workflow and are used to guide the direction and magnitude of localised velocity updates.

Calibration to the single well located within the survey area is performed after an initial pass of tomography. The anisotropic parameters delta and epsilon are estimated at the well location and extrapolated across the extent of the survey area using interpreted Eocene and Top Chalk horizons as constraints. From this point, all migrations are run as tilted-transverse isotropy (TTI). The resulting tomography-driven velocity model is shown overlain on the migrated data in Figure 4.

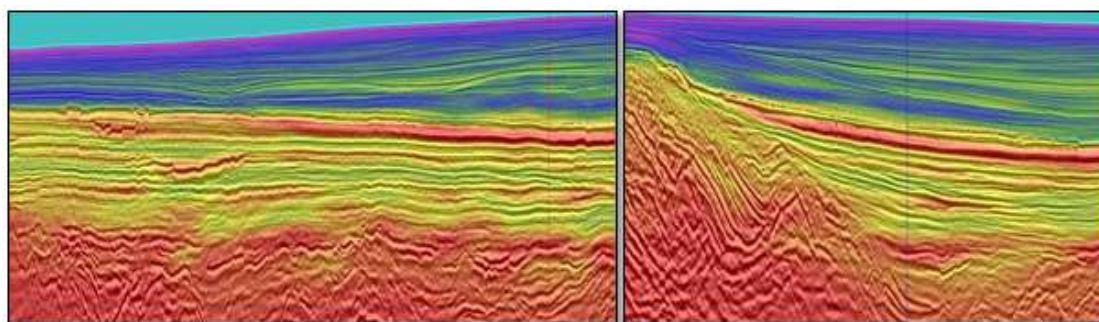


**Figure 4:** Crossline (left) and inline (right) velocity model overlay after four passes of tomography

## Full Waveform Inversion (FWI)

Tomography resolves large-scale velocity variations, but in the shallower water to the north of the survey area, several small-scale channel features are identified, cutting through the shallow sediments. Distortions in the underlying sediments implied a relatively fast velocity infill. Due to the shallow depth and very limited lateral extent of these events, diving-wave FWI is utilised to build a more detailed velocity model than is achievable with tomography alone.

The calibrated tomography model is used as the input velocity model. With limited well control in the area it is necessary to first invert for epsilon, as this is seen to stabilise later velocity updates. Using the relationship observed from the well to the south, a ratio is calculated to convert this inverted epsilon value to delta. After subsequent velocity updates another epsilon inversion is run based on the updated velocity model, which better estimates the background anisotropy. Image-guided smoothing and  $\kappa x$ - $\kappa y$  footprint removal are incorporated into the workflow to separate the acquisition footprint from the geologically driven variations in the velocity model.

The detailed channel structures are clearly seen in the resulting velocity model (Figure 5). Correctly resolving these relatively high-velocity channel infills removes undulations in the underlying sediments, allowing a more accurate interpretation. Anomalies resulting from a number of gas clouds to the south of the survey area are also detected by the FWI and the deflections in the underlying sediments are reduced, further improving the accuracy of the positioning of events and hence their interpretability.



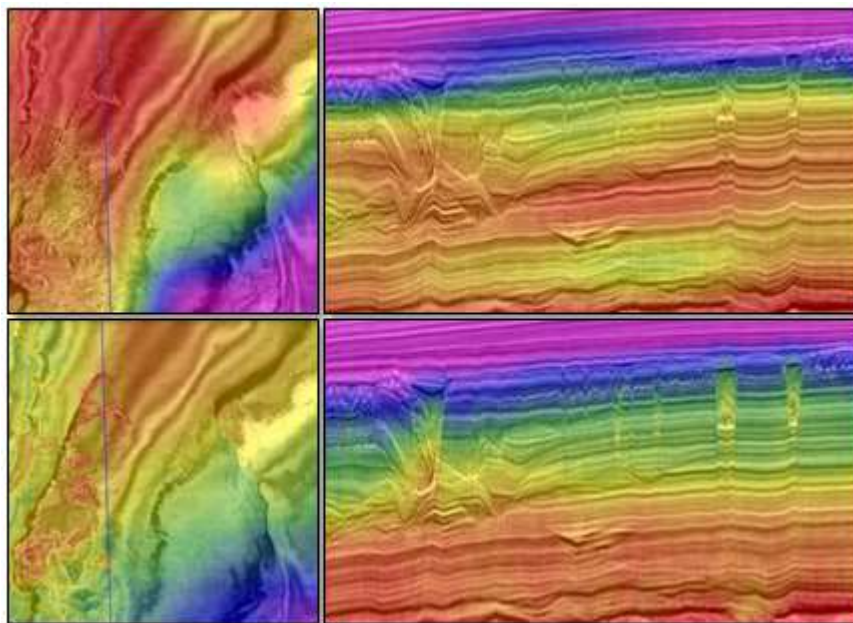


**Figure 5:** Velocity model – depth slice and crossline section before and after FWI

## Conclusions

Improved imaging of the complex and potentially prospective structures found within the Porcupine Basin is achieved through a combination of triple-source acquisition, time processing (deblend, SRME and 4D ALFT regularisation) and depth-velocity model building (IGT and FWI).

Deblending of triple-source acquisition provides a dense processing grid. This improves the SRME multiple prediction, as does regularising the input data used to create the multiple models. 4D ALFT regularisation provides accurate reconstruction of missing traces and preserves dips present on regularised traces. Detailed anomalies such as shallow channels and gas clouds are corrected with a combination of high-resolution tomography and FWI, which gives increased confidence in the positioning of events along the underlying sediments.

## Acknowledgements

The authors would like to thank Guy Hilburn for help with the tomography model building and Jian Mao for help with the FWI model building. Bent Erland Kjølhamar and Reidun Myklebust for the geological overview. Thanks to all of our colleagues who have worked on this data over the past couple of years. We'd also like to thank Connie VanSchuyver and Simon Baldock for proofreading this abstract and TGS for permission to present this data.

## References

- Baldock, S., Masoomzadeh, H., Ratnett, N., Liu, Z., O'Keefe, S., Drewell, S. and Travis, T. [2018] Deblending Of Large 3D Surveys Acquired with Triple Sources in NW Europe. 80<sup>th</sup> EAGE Conference & Exhibition, Extended Abstracts, Th P1 08.
- Berkhout, A.J. and Verschuur, D.J. [1997] Estimation of multiple scattering by iterative inversion, Part I: Theoretical considerations. *Geophysics*, **62**, 1586-1595, <https://doi.org/10.1190/1.1444261>
- Whiteside, W., Guo, M., Sun, J. and Wang, B. [2014] 5D data regularisation using enhanced antileakage Fourier transform. 84<sup>th</sup> Annual International Meeting, SEG, Expanded Abstracts, 3616-3620, <https://dx.doi.org/10.1190/segam2014-0724.1>